Carbohydrate Polymers 89 (2012) 124–131

Contents lists available at SciVerse ScienceDirect

Carbohydrate Polymers

journal homepage: www.elsevier.com/locate/carbpol

pH- and glucose-sensitive glycopolymer nanoparticles based on phenylboronic acid for triggered release of insulin

Yanxia Wang, Xinge Zhang*, Yucai Han, Cui Cheng, Chaoxing Li*

Key Laboratory of Functional Polymer Materials Ministry of Education, Institute of Polymer Chemistry, Nankai University, 94# Weijin Road, Tianjin 300071, China

ARTICLE INFO

Article history:
Received 29 July 2011
Received in revised form 3 October 2011
Accepted 21 February 2012
Available online 1 March 2012

Keywords:
Atom transfer radical polymerization
pH-sensitivity
Glucose-sensitivity
Insulin release

ABSTRACT

Amphiphilic poly(acrylic acid-*co*-acrylamidophenylboronic acid)-*block*-poly(2-acryloxyethyl galactose)-*block*-poly(acrylic acid-*co*-acrylamidophenylboronic acid) (((PAA-*co*-PAAPBA)-*b*-)$_2$PAEG) copolymer was fabricated: The poly(2-acryloyloxyethyl pentaacetylgalactoside) (PAE*Ac*G) with narrow molecular weight distributions ($M_w/M_n \leq 1.22$) was prepared by atom transfer radical polymerization (ATRP) using dibromo-p-xylene (DBX) as initiator. Then the well-defined triblock copolymer poly(*t*-butyl acrylate)-*b*-poly(2-acryloyloxyethyl pentaacetylgalactoside)-*b*-poly(*t*-butyl acrylate) (P*t*BA-*b*-PAE*Ac*G-*b*-P*t*BA) was synthesized by ATRP of *t*BA using PAE*Ac*G homopolymer with dibromo end groups as macroinitiator. After hydrolysis of *t*-butyl acrylate block, amide linkage and deacetylation, the final copolymer ((PAA-*co*-PAAPBA)-*b*-)$_2$PAEG was obtained. Because of characteristics of three different segments, amphiphilic ((PAA-*co*-PAAPBA)-*b*-)$_2$PAEG can self-assemble into pH- and glucose-responsive nanoparticles studied by dynamic light scattering (DLS) and transmission electron microscopy (TEM). Furthermore, the in vitro release profiles of insulin also revealed obvious pH- and glucose-sensitivity of the nanoparticles. The analysis of cell viability suggested that the copolymer nanoparticles had good cytocompatibility.

1. Introduction

Stimuli-responsive polymers have received much attention in the last years because of their use in areas such as drug and gene delivery, tissue engineering and biosensors (Bae, Fukushima, Harada, & Kataoka, 2003; Ganta, Devalapally, Shahiwala, & Amiji, 2008; Reppy & Pindzola, 2007; Rijcken, Soga, Hennink, & Nostrum, 2007; Xue et al., 2009). They undergo abrupt physical or chemical change in response to change of environmental conditions such as pH, temperature, light, magnetic field, and glucose (Gil & Hudson, 2004; Hernández, Chécot, Gnanou, & Lecommandoux, 2005; Lattuada & Hatton, 2007; Zhao, 2009). Poly(acrylic acid) (PAA) is one of the most studied pH-responsive polymers (Alarcon, Pennadam, & Alexander, 2005; Bajpai, Shukla, Bhanu, & Kankane, 2008; Lowe & McCormick, 2007). The sensitivity comes from the ionization of the carboxyl groups. PAA is ionized and hydrophilic at high pH, and non-ionized and hydrophobic at low pH. Polymeric micelles including PAA have been extensively studied in recent years. The pH-responsive poly(acrylic acid-*b*-DL-lactide) micelles were stable at a pH above 3.0, however, they aggregated and precipitated in the solution when further decreasing pH (Xue et al., 2009). Block copolymer PAA-*b*-P4VP formed micelles with different structures at different pH values. At low pH, polymer was protonated, micelles formed with hydrophobic PAA core and cationic polyelectrolyte P4VP shell. While at high pH, protons were released, micelles formed with hydrophobic P4VP core and anionic polyelectrolyte PAA shell (Bo & Zhao, 2006).

On the other hand, glucose is a particularly interesting target molecule owing to its inherent biological activities and physicochemical properties in living organisms. Phenylboronic acid (PBA) group has been frequently utilized to design glucose-responsive materials due to their unique reversible covalent interaction with *cis*-diol moiety in glucose to form cyclic boronate moieties. An important property of PBA in aqueous medium is that they are in equilibrium between an uncharged and a charged form (Horgan et al., 2006). The charged PBA is well known to form a stable complex with glucose in aqueous medium, which lay the foundation for the glucose-responsiveness of PBA-containing materials (Li, Larsson, Jungvid, Galaev, & Mattiasson, 2001; Winblade, Nikolic, Hoffman, & Hubbell, 2000). The block copolymer poly(3-acrylamidophenylboronic acid)-*b*-poly(*N*,*N*-dimethylacrylamide) was prepared via the RAFT polymerization of unprotected 3-acrylamidophenylboronic acid monomers, and the copolymer was responsive to glucose (Roy, Cambre, & Sumerlin, 2008). Glucose-responsive micelles from 3-aminophenyboronic acid-modified PEG-*b*-PAA copolymer were fabricated, and insulin-loaded micellar nanoparticles exhibited glucose-regulated insulin release

* Corresponding authors. Tel.: +86 22 2350 1645; fax: +86 22 2350 5598.
E-mail addresses: zhangxinge@nankai.edu.cn (X. Zhang), lcx@nankai.edu.cn (C. Li).

0144-8617/$ – see front matter © 2012 Elsevier Ltd. All rights reserved.
doi:10.1016/j.carbpol.2012.02.060

characteristics (Wang et al., 2009). However, a disadvantage of boronic acid-containing compounds is that they have some degree of cytotoxic activity (Qureshi, Al-Shabanah, Al-Harbi, Al-Bekairi, & Raza, 2001). To address this problem, it is necessary to introduce biocompatible compounds. Materials containing carbohydrate moieties as pendant groups have received more and more attention due to their biological and biomedical functions, and carbohydrates containing abundant hydroxyl groups could improve the hydrophilicity and biocompatibility of the carbohydrate-immobilized materials (Auzély-Velty, Cristea, & Rinaudo, 2002; Lamiral, Melia, & Haddleton, 2004; Xiao, Li, Liang, & Lu, 2008).

In this paper, first, phenylboronic acid functionalized glycopolymer ((PAA-*co*-PAAPBA)-*b*-)$_2$PAEG was synthesized: The PAE*Ac*G homopolymers with dibromo end groups were prepared by ATRP using dibromo-p-xylene (DBX) as initiator. The monomer conversion as a function of time, and molecular weight (M_n) and molecular weight distribution (M_w/M_n) as a function of monomer conversion were analyzed. Then, P*t*BA-*b*-PAE*Ac*G-*b*-P*t*BA triblock copolymer was prepared by subsequent ATRP using PAE*Ac*G as macroinitiator. After hydrolysis of *t*-butyl acrylate block, amide linkage and deacetylation, the final copolymer ((PAA-*co*-PAAPBA)-*b*-)$_2$PAEG was obtained. Second, we prepared ((PAA-*co*-PAAPBA)-*b*-)$_2$PAEG nanoparticles by a self-assembly process and studied the pH- and glucose-responsibility of the nanoparticles (Scheme 1) by dynamic light scattering (DLS) and transmission electron microscopy (TEM). Finally, the encapsulation behavior of the nanoparticles using the insulin as model drug and the release properties of the insulin-loaded nanoparticles under different pH values and glucose concentrations were evaluated.

2. Experimental

2.1. Materials

t-Butyl acrylate (*t*BA) (Aldrich, 98%) was distilled under reduced pressure before use. 2-*O*-acryloyloxyethyl-(2,3,4,6-*tetra*-*O*-acetyl-*β*-D-galactopyranoside) (AE*Ac*G) was prepared using a method similar to that described by our group and others (Dahmen, Frejd, Gronberg, Lave Thomas Magnusson, & Noori, 1983; Murakami, Hirono, Sato, & Furusawa, 2007). *N*,*N*′,*N*′,*N*″-Pentamethyl diethylenetriamine (PMDETA), 1-ethyl-3-(3-dimethylaminopropyl-carbodiimide) hydrochloride (EDC), 1-hydroxybenzotrizole (HOBt), and 3-[4,5-dimethylthiazol-2-yl]-2,5-diphenylterazolium bromide (MTT) were purchased from the J&K China Chemical Ltd. (Beijing, China) and used without further purification. Pure crystalline porcine insulin (with a nominal activity of 28 IU/mg) that was used without further purification was obtained from the Xuzhou Wanbang Biochemical Co., Ltd. (Jiangsu, China). The semipermeable membrane (molecular weight cutoff (MWCO) = 3500) used for dialysis was purchased from Shanghai Green Bird Science and Technology Co. Ltd. (Shanghai, China). All other solvents and reagents of the highest grade were purchased from commercial sources and were used as received, unless otherwise noted.

2.2. Synthesis of poly(acrylic acid-co-acryl amidophenylboronic acid)-block-poly(2-acryloxyethyl galactose)-block-poly(acrylic acid-co-acryl amidophenylboronic acid) (((PAA-co-PAAPBA)-b-)$_2$PAEG) copolymer

((PAA-*co*-PAAPBA)-*b*-)$_2$PAEG copolymer was synthesized as follows: First PAE*Ac*G homopolymer was prepared by ATRP of AE*Ac*G using DBX as initiator, with bipy as the ligand in conjunction with CuBr in chlorobenzene at 80 °C. The tubers were removed at predetermined intervals for kinetic and gel permeation chromatography (GPC) analysis (Dong, Sun, Faucher, Apkarian, & Chaikof, 2004; Li, Liang, Chen, & Li, 2000; Liang, Li, Chen, & Li, 1999). Then, P*t*BA-*b*-PAE*Ac*G-*b*-P*t*BA triblock copolymer was prepared by subsequent ATRP at 90 °C under nitrogen in a solvent mixture of butanone and 2-propanol (7:3, v/v) using PAE*Ac*G as macroinitiator and a CuBr/PMDETA catalyst/ligand system (Storey, Scheuer, & Achord, 2005).

In the next step, poly(acrylic acid)-*b*-poly(2-acryloyloxyethyl pentaacetylgalactoside)-*b*-poly(acrylic acid) (PAA-*b*-PAE*Ac*G-*b*-PAA) was prepared by hydrolyzing P*t*BA-*b*-PAE*Ac*G-*b*-P*t*BA in CH_2Cl_2 with trifluoroacetic acid at room temperature for 24 h (Lu, Liu, & Duncan, 2005; Tian, Ravi, Bromberg, Hatton, & Tam, 2007). Then, the carboxylic acid group of PAA-*b*-PAE*Ac*G-*b*-PAA reacted with the amino group of 3-aminophenylboronic acid (APBA) monohydrate to form poly(acrylic acid-*co*-acryl amidophenylboronic acid)-*block*-poly(2-acryloyloxyethyl pentaacetylgalactoside)-*block*-poly(acrylic acid-*co*-acryl amidophenylboronic acid) (((PAA-*co*-PAAPBA)-*b*-)$_2$PAE*Ac*G) copolymer by the amide linkage. The coupling reaction was carried out in dimethylformamide at room temperature in the presence of EDC and HOBt (Wang et al., 2009). Finally, the deacetylation of ((PAA-*co*-PAAPBA)-*b*-)$_2$PAE*Ac*G copolymer was achieved by treatment with hydrazine monohydrate in dimethyl sulfoxide (DMSO) and H_2O (4:1, v/v) at room temperature (Dong, Faucher, & Chaikof, 2004; Tsutsumiuchi, Aoi, & Okada, 1997).

2.3. Preparation and characterization of the nanoparticles

((PAA-*co*-PAAPBA)-*b*-)$_2$PAEG nanoparticles were prepared by the nanoprecipitation method. Briefly, 5 mg of amphiphilic block copolymer was dissolved in 1 mL of a mixed solvent of DMSO and H_2O (4:1, v/v) and was added dropwise to water under stirring. The resulting suspension was stirred for an additional 30 min and was then dialyzed. The suspension was analyzed as is or freeze-dried for further characterization.

In order to study the pH sensitivity of nanoparticles, the nanoparticles were prepared with varying pH values adjusted by either 0.1 M NaOH or HCl. The hydrodynamic diameter (D_H), polydispersity index (PDI) and zeta potential of the nanoparticles were determined by dynamic light scattering analyzer (Malvern, Nano ZS90/ZEN3690). Furthermore, the D_H and PDI of the nanoparticles, before and after the treatment with 1 and 3 mg/mL glucose, were also determined by dynamic light scattering (DLS). The measurement was carried out at 25 °C in aqueous solution of pH 7.4, with the exception of one array of samples, which were analyzed at pH 9.0. The data reported herein represented an average of at least triplicate measurements.

The morphology of nanoparticles was examined by transmission electron microscopy (TEM, Philips EM400ST). The TEM samples were prepared by placing a few drops of nanoparticle suspension on a 300-mesh copper grid covered with carbon and allowed to stand for 20 s. Excess solutions on the grid were gently removed with absorbent paper. The samples were then dried for 2 days.

2.4. Encapsulation of insulin

To assess the potential use of these nanoparticles as drug delivery system, insulin was chosen to study the encapsulation behavior of the nanoparticles. Insulin (5 mg) was dissolved in 10 mL of distilled water, then ((PAA-*co*-PAAPBA)-*b*-)$_2$PAEG copolymer solution was added slowly to insulin solution under stirring. The insulin-loaded nanoparticles were obtained by centrifugation at 11000 rpm for 30 min and washed with distilled water three times. The amount of free insulin in the supernatant was measured by the Bradford method using a UV spectrometer (Shimadzu, UV-2550) at 595 nm.

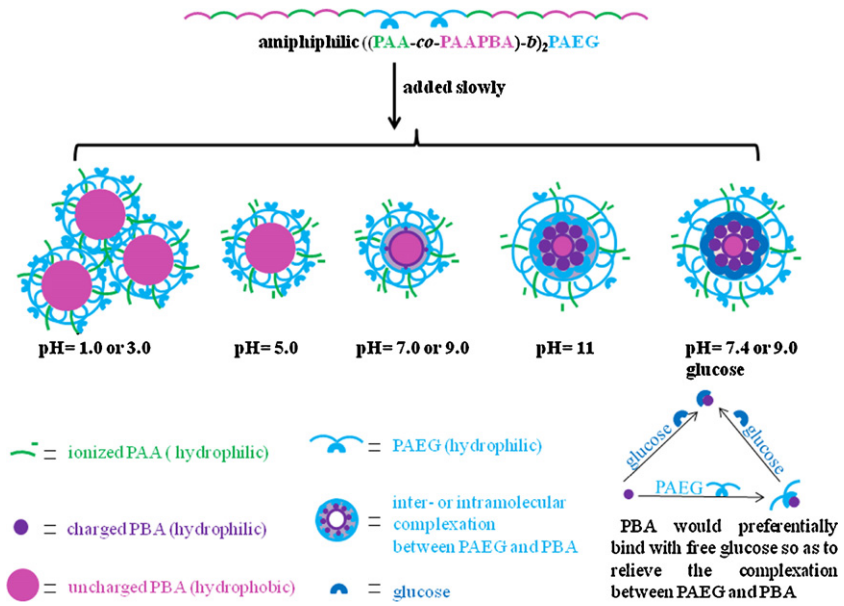

Scheme 1. Schematic illustration of the pH- and glucose-responsive self-assembly of ((PAA-*co*-PAAPBA)-*b*-)$_2$PAEG copolymer.

Insulin entrapment efficiency (EE) and loading capacity (LC) were calculated using the following equations:

$$EE\% = \frac{\text{total insulin} - \text{free insulin}}{\text{total insulin}} \times 100$$

$$LC\% = \frac{\text{total insulin} - \text{free insulin}}{\text{nanoparticles weight}} \times 100$$

All measurements were performed in triplicate and averaged.

2.5. In vitro release studies

Insulin release was analyzed by incubating insulin-loaded ((PAA-*co*-PAAPBA)-*b*-)$_2$PAEG nanoparticles in different pH value solutions with different glucose concentrations at 37 °C while shaking (100 rev/min). At appropriate time points, 100 μL supernatant was withdrawn and fresh solution was replenished. The amount of free insulin was determined by the Bradford assay. A calibration curve was made using blank nanoparticles in order to correct for the intrinsic absorption of the polymer. In each experiment, the samples were analyzed in triplicate and the error bars in the plot represented the standard deviation.

2.6. Cell viability

Cell viability was evaluated by using CHO cells. The cell line was cultured in Dulbecco's modified Eagle's medium (DMEM) in 5% CO_2, 95% O_2. The cells were seeded on to 96-well plates at 10,000 cells per well. Cells were allowed to grow until cell monolayers were obtained. The copolymers were dissolved in a mixed solvent of DMSO and H_2O (4:1, v/v). After removal of the organic solvent by dialysis, the resulting solution was diluted with culture medium to give a final range of concentrations from 50 to 500 μg/mL. The medium from each well was replaced with 100 μL of the copolymer solution. The plates were incubated at 37 °C in 5% CO_2 for 24 h. Each sample was plated in five replicates per plate. After 2 and 4 days, the culture medium and 10 μL of MTT were used to replace the mixture in each well. The cells were incubated for another 4 h in 5% CO_2 at 37 °C prior to removal of the culture medium and MTT. Isopropanol (100 μL) was added to each well to dissolve the formazan crystals that formed in response to MTT exposure. Plates were incubated in 5% CO_2 at 37 °C for 10 min and at 6 °C for 15 min prior to determination of optical density using a microplate reader at 570 nm. Relative cell proliferation rate was determined as a percentage of the negative control; untreated cells were used as the negative control and their proliferation rate was set to 100%.

3. Results and discussion

3.1. Synthesis and characterization of ((PAA-co-PAAPBA)-b-)$_2$PAEG copolymer

((PAA-*co*-PAAPBA)-*b*-)$_2$PAEG copolymer was synthesized via sequential ATRP and amide linkage. First, PAE*Ac*G homopolymer was prepared by ATRP of AE*Ac*G using DBX as initiator. Fig. S2A shows the first-order plot for the ATRP polymerization of AE*Ac*G. It can be seen that polymerization took place smoothly. However, deviations from the linear line were observed at higher conversions. This might be attributed to the decreasing concentration of active species with the polymerization system over time. It was clear that this represented a relative increase in the rate of termination. Fig. S2B is the dependence of M_n and M_w/M_n of the obtained polymer on the polymerization conversion. It can be seen that *M*n increased linearly with the polymerization conversion. This figure also shows that the polymerization resulted in low M_w/M_n, which was typical for all polymerization. As monomer conversion increased, the M_w/M_n increased slightly, suggesting termination activity, which was inherent in free radical polymerizations. Furthermore, the PAE*Ac*G homopolymers with different molecular weights were synthesized by changing the mole ratio of monomer to initiator. As listed in Table S1, $M_{n,NMR}$ was in agreement with $M_{n,theo}$ and $M_{n,GPC}$. The GPC curves for the ATRP of AE*Ac*G are shown in Fig. S3A and B. All told, these results indicate that the ATRP of AE*Ac*G monomer was of a controlled/"living" radical polymeriazation and well defined PAE*Ac*G homopolymers with dibromo end groups were obtained. Then, P*t*BA-*b*-PAE*Ac*G-*b*-P*t*BA triblock copolymer was prepared by subsequent ATRP using PAE*Ac*G as macroinitiator. When PAE*Ac*G macroinitiator was low molecular weight (Table S2), the $M_{n,GPC}$ and $M_{n,theo}$ of P*t*BA-*b*-PAE*Ac*G-*b*-P*t*BA were very approximate, demonstrating high initiation efficiency. However, for PAE*Ac*G macroinitiator with high molecular weight (Table S2), the M_n of P*t*BA-*b*-PAE*Ac*G-*b*-P*t*BA by GPC was higher

Table 1
The physicochemical properties of ((PAA-*co*-PAAPBA)-*b*-)$_2$PAEG nanoparticles.

Sample	Insulin concentration (mg/mL)	D_H (nm)	PDI	Zeta potential (mV)	EE (%)	LC (%)
((PAA$_{28}$-*co*-PAAPBA$_{38}$)-*b*-)$_2$PAEG$_{11}$	0	224.5 ± 0.9	0.36 ± 0.009	−31.2 ± 1.19	–	–
	0.5	232.2 ± 1.2	0.32 ± 0.023	−33.0 ± 0.70	57.00 ± 1.40	35.62 ± 0.89
((PAA$_{19}$-*co*-PAAPBA$_{47}$)-*b*-)$_2$PAEG$_{11}$	0	214.5 ± 0.7	0.23 ± 0.017	−22.6 ± 1.16	–	–
	0.5	221.6 ± 0.9	0.25 ± 0.021	−25.6 ± 0.27	50.21 ± 0.40	29.37 ± 0.35
((PAA$_{13}$-*co*-PAAPBA$_{53}$)-*b*-)$_2$PAEG$_{11}$	0	270.2 ± 1.2	0.19 ± 0.007	−26.7 ± 0.96	–	–
	0.5	280.2 ± 1.3	0.18 ± 0.015	−31.9 ± 0.71	45.87 ± 0.40	20.34 ± 0.54

than expected. It was known that not all PAE*Ac*G homopolymers obtained by the ATRP using DBX as initiator were terminated on both ends by bromine, and some side reactions were possible on the terminal bromo groups during the polymerization of *t*BA. Fig. S3C shows the GPC curves of the macroinitiators and triblock copolymers. As can be observed in the figure, an obvious shift was found through the copolymerization, and these curves were monomodal. Taken together these data indicate a degree of control for the ATRP of *t*BA using PAE*Ac*G macroinitiators.

In the next step, PAA-*b*-PAE*Ac*G-*b*-PAA was prepared by hydrolyzing P*t*BA-*b*-PAE*Ac*G-*b*-P*t*BA. Then, the carboxylic acid group of PAA-*b*-PAE*Ac*G-*b*-PAA reacted with the amino group of APBA monohydrate to form ((PAA-*co*-PAAPBA)-*b*-)$_2$PAE*Ac*G copolymer by the amide linkage. As shown in Table S3, ((PAA-*co*-PAAPBA)-*b*-)$_2$PAE*Ac*G copolymers with different degrees of modification such as 76, 94 and 106 were synthesized. Finally, the deacetylation of ((PAA-*co*-PAAPBA)-*b*-)$_2$PAE*Ac*G copolymer was successfully achieved by treatment with hydrazine monohydrate in DMSO and H_2O (4:1, v/v) at room temperature. Thus, sequential ATRP and coupling reaction provide a facile approach for the synthesis of amphiphilic ((PAA-*co*-PAAPBA)-*b*-)$_2$PAEG.

3.2. Characterization of blank and insulin-loaded nanoparticles

The PAEG and PAA segments were soluble in neutral solution, and the PAAPBA segment was insoluble in acidic or neutral solution. Therefore, the nanoparticles self-assembled by amphiphilic ((PAA-*co*-PAAPBA)-*b*-)$_2$PAEG had a core–shell structure with a hydrophobic core composed of PAAPBA and hydrophilic shell composed of PAEG and PAA in the aqueous solution at pH 7.0, and the complexation of PBA with the galactose moieties in PAEG also promoted the self-assembly (Scheme 1).

According to DLS measurement, the mean size of blank nanoparticles was in range of 230 to 270 nm with narrow distribution (Table 1). The zeta potentials of ((PAA-*co*-PAAPBA)-*b*-)$_2$PAEG nanoparticles were about −25 mV (Table 1), which was attributed to charged phenylboronic acid and deprotonated carboxylic group of copolymer.

Insulin with random sequenced hydrophilic and hydrophobic amino acid in the linear chain can self-assemble with the amphiphilic glycopolymers due to hydrophilic and hydrophobic interaction. The insulin-loaded ((PAA-*co*-PAAPBA)-*b*-)$_2$PAEG nanoparticles were prepared by the self-assembly process. The mean size of the nanoparticles became greater after the drug loading (Table 1). In addition, the surface charge of insulin-loaded nanoparticles was more negative than that of blank nanoparticles. This was due to the net negative charge of insulin (p*I* 5.3) in pH 7.0 aqueous solution. The results also show that EE and LC increased with increasing hydrophilic content, and the LC was more than 20% for the three nanoparticles (Table 1).

3.3. pH-sensitivity of nanoparticles

It is well-known that PAA chain and PAAPBA segment undergo magnificent conformation changes as the pH value increases. Therefore, it is interesting to study pH-sensitivity of nanoparticles. The D_H and zeta potential of nanoparticles in aqueous solution with different pH values were characterized by DLS (Table 2). The aggregation and precipitation of the nanoparticles were observed at pH 1.0 and 3.0, which can be attributed to the complexation between PAA and PAEG through the hydrogen bonding interaction between the carboxyl groups of PAA (pK_a = 4.7) and hydroxyl groups of PAEG. The hydrophilic-hydrophobic balance was shifted toward hydrophobicity, resulting in aggregation of the nanoparticles. However, the nanoparticles were stable at pH 5.0, 7.0 and 9.0 with negative charge, and little change in the size of the nanoparticles had been found. This was due to that PAA had been totally ionized at these pH values. In addition, as the pH value increased, the zeta potential became more negative. It was possible that the more interactions between PBA and galactose moieties in PAEG at higher pH values, the easier the shift of the equilibrium to the direction of negative charged forms. A further increase of the pH value to 11 resulted in the pronounced increase of the nanoparticle size. The high pH can enhance the ionization degree of boronic acid (pK_a = 8.2), as indicated by the zeta potential of the nanoparticles at pH 11 (the zeta potential tests revealed that the zeta potential of the nanoparticles at this pH was most negative). As a result, the charge repulsion in the nanoparticles increased, leading to the swelling of nanoparticles. Furthermore, Fig. 1 shows the TEM image of ((PAA$_{28}$-*co*-PAAPBA$_{38}$)-*b*-)$_2$PAEG$_{11}$ nanoparticles at pH 7.0 (Fig. 1A) and 11 (Fig. 1B), and the nanoparticles had a spherical shape. A dramatic increase in the size at pH 11 was observed, which was in good agreement with DLS results. These data indicate that the nanoparticles exhibit pH-responsive property.

3.4. Glucose-sensitivity of nanoparticles

The introduction of PBA made the nanoparticles glucose-sensitive. It was necessary to study the glucose-sensitivity of the nanoparticles. Table 3 shows the D_H and PDI of nanoparticles in aqueous solution of pH 7.4 and 9.0 with different glucose concentrations measured at 25 °C. Even after glucose treatment, there was

Table 2
D_H, PDI and zeta potential of ((PAA$_{28}$-*co*-PAAPBA$_{38}$)-*b*-)$_2$PAEG$_{11}$ nanoparticles at different pH values measured by DLS.

pH value	D_H (nm)	PDI	Zeta potential (mV)
1.0	Precipitation	Precipitation	Precipitation
3.0	Precipitation	Precipitation	Precipitation
5.0	230.4 ± 4.39	0.33 ± 0.074	−24.7 ± 0.25
7.0	224.6 ± 1.55	0.29 ± 0.011	−25.5 ± 0.46
9.0	239.7 ± 1.96	0.24 ± 0.005	−25.9 ± 0.008
11	307.3 ± 2.63	0.26 ± 0.038	−30.5 ± 3.160

Table 3
D_H and PDI of the nanoparticles at various glucose concentrations measured by DLS.

Sample	pH Value	Glucose concentration (0 mg/mL) D_H (nm)/PDI	Glucose concentration (1 mg/mL) D_H(nm)/PDI	Glucose concentration (3 mg/mL) D_H (nm)/PDI
((PAA$_{28}$-*co*-PAAPBA$_{38}$)-*b*-)$_2$PAEG$_{11}$	9.0	239.7/0.24	271.2/0.27	338.6/0.30
((PAA$_{28}$-*co*-PAAPBA$_{38}$)-*b*-)$_2$PAEG$_{11}$	7.4	228.9/0.36	235.5/0.32	241.9/0.29
((PAA$_{19}$-*co*-PAAPBA$_{47}$)-*b*-)$_2$PAEG$_{11}$	7.4	215.9/0.23	224.0/0.25	228.7/0.25
((PAA$_{13}$-*co*-PAAPBA$_{53}$)-*b*-)$_2$PAEG$_{11}$	7.4	288.2/0.19	297.2/0.18	304.1/0.22

a narrow size distribution, with the PDI ranging from 0.19 to 0.36 for all the samples analyzed. The ((PAA$_{28}$-*co*-PAAPBA$_{38}$)-*b*-)$_2$PAEG$_{11}$ nanoparticle size expanded dramatically with an increase in glucose concentration at pH 9.0. In the absence of glucose, the D_H was only 257.7 nm. However, the nanoparticles swelled to nearly 80 nm in size when glucose concentration was 3 mg/mL. As shown in Fig. 2, after glucose treatment, the nanoparticles had a compact core surrounded by a fluffy coat, and the size increased obviously. These were due to the glucose-sensitivity of the PBA in nanoparticles. The PBA group shifted the ionization equilibrium toward the charged form when complexation with free glucose occurred around the pK_a (pK_a = 8.2), which caused nanoparticles swelling. We repeated the same experiment at pH 7.4 and observed that the D_H values of the nanoparticles after treatment with 1 and 3 mg/mL of glucose were slightly greater than that without glucose. The coordination between the carboxylate anion and PBA can reduce the pK_a of the PBA (Wang et al., 2010). As a result, the ((PAA-*co*-PAAPBA)-*b*-)$_2$PAEG nanoparticles showed a degree of sensitivity to glucose at pH 7.4.

3.5. In vitro release of insulin

Fig. 3A shows the release profiles of insulin from drug-loaded nanoparticles in pH 1.0 HCl solution and pH 7.4 phosphate buffer solution without glucose. At pH 1.0, the burst release of insulin occurred during the initial 2 h, and 73% of insulin was released. At this pH, the hydrogen bonding interaction between the carboxyl groups of PAA (pK_a = 4.7) and hydroxyl groups of PAEG was strengthened. And, the interaction between PBA and galactose moieties in PAEG was weakened. These may result in that the interaction between insulin and polymers was weakened and insulin was released from nanoparticles. Additionally, the good solubility

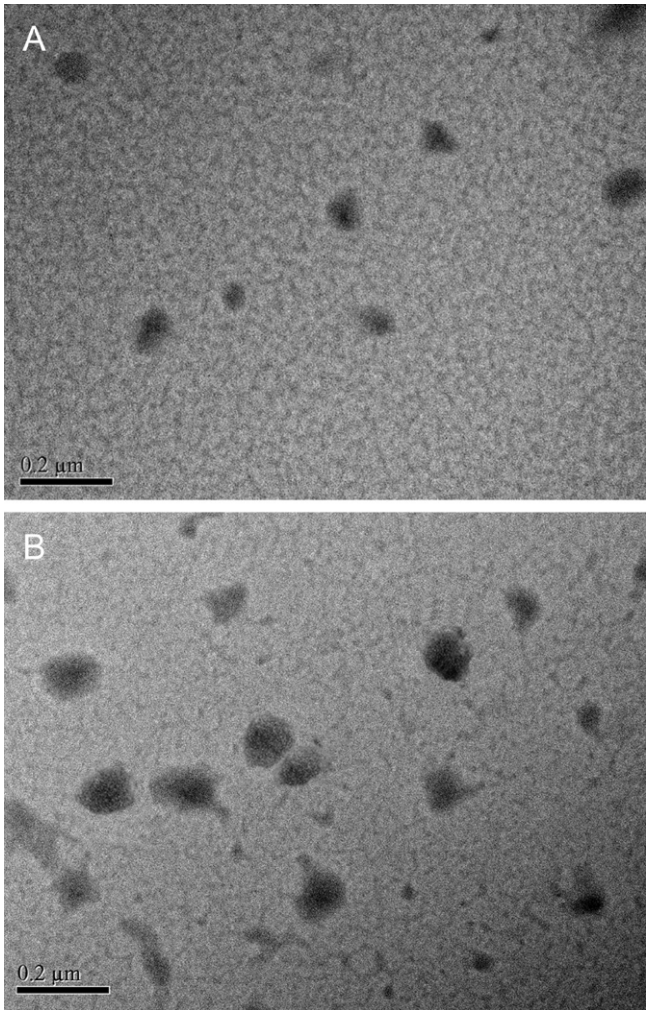

Fig. 1. TEM micrograph of ((PAA$_{28}$-*co*-PAAPBA$_{38}$)-*b*-)$_2$PAEG$_{11}$ nanoparticles at pH 7.0 (A) and pH 11 (B).

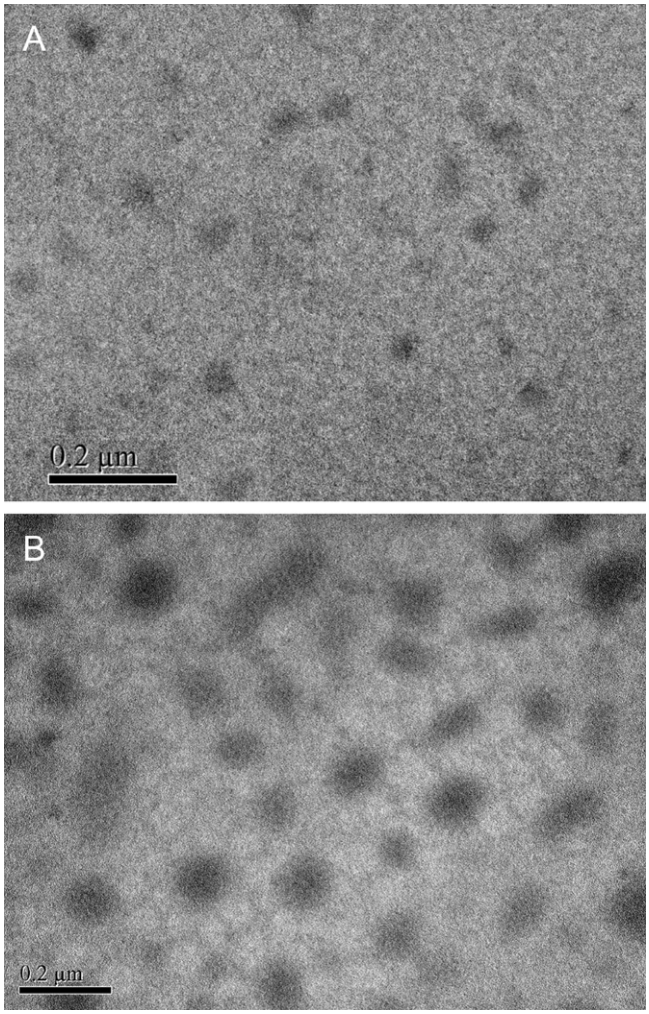

Fig. 2. TEM micrograph of ((PAA$_{28}$-*co*-PAAPBA$_{38}$)-*b*-)$_2$PAEG$_{11}$ nanoparticles before (A) and after (B) treatment with 3 mg/mL glucose at pH 9.0.

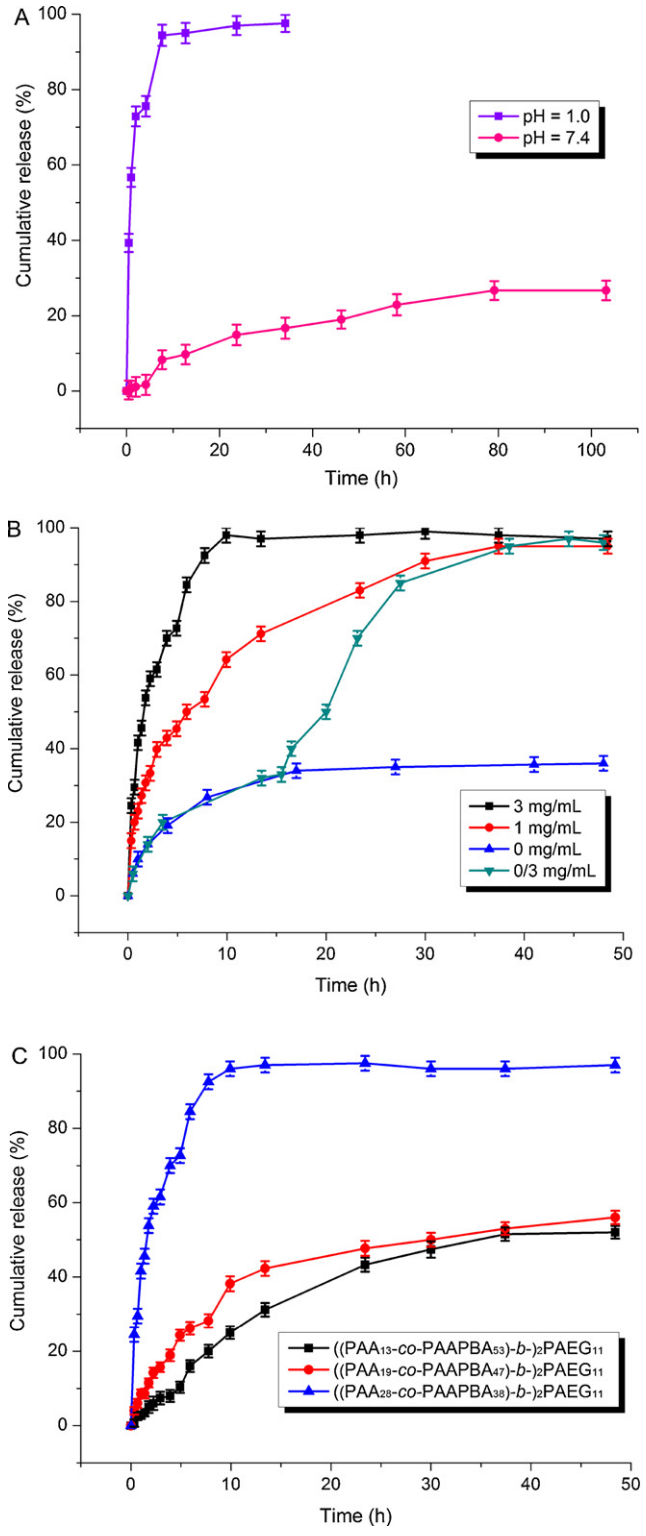

Fig. 3. In vivo release profiles of insulin. (A) In vitro release profiles from $((PAA_{13}\text{-}co\text{-}PAAPBA_{53})\text{-}b\text{-})_2PAEG_{11}$ nanoparticles at pH 1.0 and 7.4; (B) In vitro release profiles from $((PAA_{28}\text{-}co\text{-}PAAPBA_{38})\text{-}b\text{-})_2PAEG_{11}$ nanoparticles at various glucose concentrations; (C) In vitro release profiles of insulin from $((PAA\text{-}co\text{-}PAAPBA)\text{-}b\text{-})_2PAEG$ nanoparticles at a glucose concentration of 3 mg/mL.

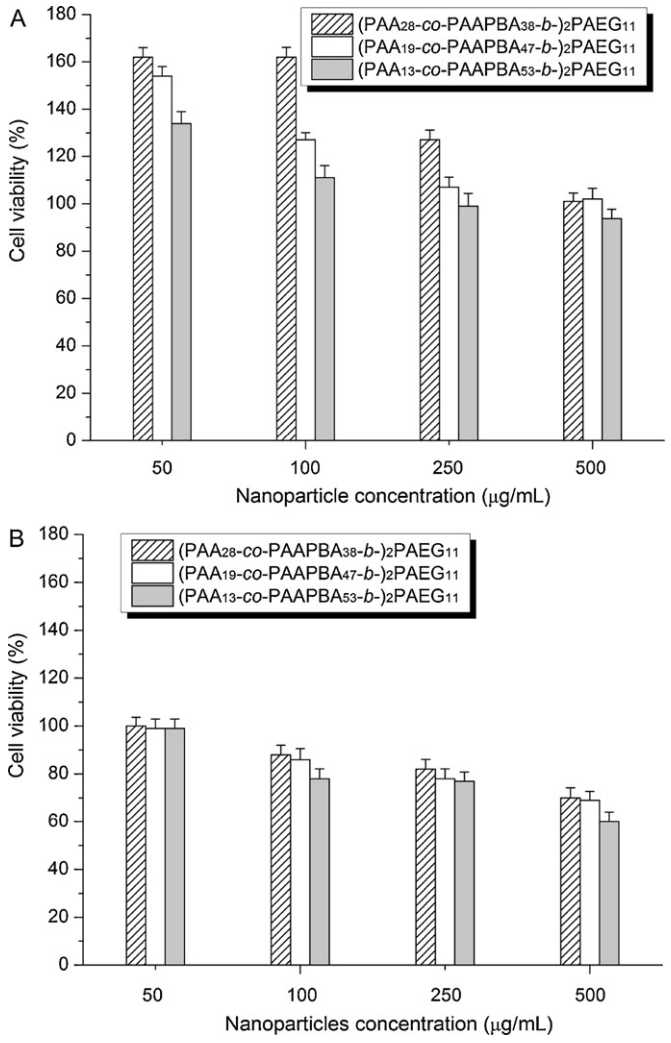

Fig. 4. Cell viability after incubation as function of nanoparticles concentration by MTT assay, at 37 °C for (A) 2 days and (B) 4 days.

of insulin and PAA at pH 1.0 led to more insulin release. Within 8 h, 95% insulin was released followed by the establishment of a plateau phase. In contrast, a maximum of only 26.7% insulin could be released within 103 h at pH 7.4. The nanoparticles were stable at pH 7.4, so the hydrophilic and hydrophobic interaction between amphiphilic glypolymers and insulin may retard insulin release. Most importantly, the poor solubility of insulin at this pH resulted in a certain amount of insulin staying in the nanoparticles.

Fig. 3B shows the cumulative release profiles of insulin in response to different concentrations of glucose at pH 7.4. The results indicate a burst release phase for all glucose concentrations was examined within 3 h. After the first couple of hours, insulin was gradually released from the nanoparticles. The burst release without glucose corresponded to the diffusion of insulin located on the nanoparticle surfaces. In the medium containing glucose, the burst of insulin was much higher, with 40% and 60% of the insulin being released following treatment with 1 and 3 mg/mL of glucose, respectively, compared to 17% insulin release in nanoparticles incubated in glucose-free medium. The amounts of insulin released after 13 h for each glucose concentration were 30%, 71%, and 97%, respectively. Another study on release profile of $((PAA_{28}\text{-}co\text{-}PAAPBA_{38})\text{-}b\text{-})_2PAEG_{11}$ nanoparticles was conducted by changing the glucose concentration from 0 to 3 mg/mL in the same medium. The rapid release occurred after 15.5 h was for glucose-sensitive release. These results suggest that the

nanoparticles were responsive to glucose and released insulin rapidly upon exposure to glucose.

Fig. 3C shows the release profile of insulin in the medium of the same glucose concentration (3 mg/mL) at pH 7.4. Insulin was released from the nanoparticles in the following order: ((PAA$_{28}$-*co*-PAAPBA$_{38}$)-*b*-)$_2$PAEG$_{11}$ > ((PAA$_{19}$-*co*-PAAPBA$_{47}$)-*b*-)$_2$PAEG$_{11}$ > ((PAA$_{13}$-*co*-PAAPBA$_{53}$)-*b*-)$_2$PAEG$_{11}$, and the cumulative amounts of insulin released after 30 h for each nanoparticles were 78%, 56% and 47%, respectively. The nanoparticles became swollen after glucose exposure, which resulted in a rapid release of insulin. Furthermore, the more the hydrophilic segments in ((PAA-*co*-PAAPBA)-*b*-)$_2$PAEG copolymer, the easier it was for the glucose to access and penetrate the nanoparticles and react with PBA.

3.6. Cell viability

Most of the boronated moieties and their derivatives have cytotoxic activity (Alarcon et al., 2005). Therefore, it was important to verify the harmless nature of the nanoparticles. As shown in Fig. 4A, it was found that the cell viability of CHO cells was maintained over 80% with different concentrations of nanoparticles (from 50 to 500 μg/ml) for 2 days. However, the cell viability decreased clearly after incubated for 4 days (Fig. 4B). After treatment with the three nanoparticles for 2 days or 4 days, the cell viability was in the following order: ((PAA$_{28}$-*co*-PAAPBA$_{38}$)-*b*-)$_2$PAEG$_{11}$ > ((PAA$_{19}$-*co*-PAAPBA$_{47}$)-*b*-)$_2$PAEG$_{11}$ > ((PAA$_{13}$-*co*-PAAPBA$_{53}$)-*b*-)$_2$PAEG$_{11}$. It was clear that the cell viability increased slightly as the carbohydrate moieties in the copolymer increased. The reduction of the cytotoxicity of PBA was mainly attributed to the introduction of the carbohydrate moieties, which was in agreement with the results reported by Jin et al. (2009). A possible mechanism for these was that hydrophilic sugar containing hydroxide groups covered the PBA, thus reducing the interaction between PBA and the cells. The copolymers containing more PAEG segment have the potential for in vivo use.

4. Conclusions

In this study, amphiphilic ((PAA-*co*-PAAPBA)-*b*-)$_2$PAEG copolymer was fabricated and self-assembled into pH- and glucose-sensitive nanoparticles. At pH 1.0 and 3.0, the aggregation and precipitation of the nanoparticles was observed. The nanoparticles were stable at pH 5.0, 7.0 and 9.0 with negative charge (∼−25 mV). The particle size increased significantly as pH increased to 11. Moreover, the glucose-responsive behavior of ((PAA-*co*-PAAPBA)-*b*-)$_2$PAEG nanoparticles was dependent on the pH value. The sensibility of the nanoparticles to glucose was stronger at pH 9.0 than pH 7.4. Insulin release profiles also revealed that the release of insulin was in correlation with pH value and glucose concentration. Additionally, cell viability suggested the copolymer nanoparticles have good cytocompatibility.

Acknowledgment

This work was supported by the National Science Foundation of China (grant no. 20804021 and 51173085).

Appendix A. Supplementary data

Supplementary data associated with this article can be found, in the online version, at doi:10.1016/j.carbpol.2012.02.060.

References

Alarcon, C. H., Pennadam, S., & Alexander, C. (2005). Stimuli responsive polymers for biomedical applications. *Chemical Society Reviews*, *34*, 276–285.

Auzély-Velty, R., Cristea, M., & Rinaudo, M. (2002). Galactosylated *N*-vinylpyrrolidone-maleic acid copolymers: synthesis, characterization, and interaction with lectins. *Biomacromoleculars*, *3*, 998–1005.

Bae, Y., Fukushima, S., Harada, A., & Kataoka, K. (2003). Design of environment-sensitive supramolecular assemblies for intracellular drug delivery: polymeric micelles that are responsive to intracellular pH change. *Angewandte Chememie International Edition*, *42*, 4640–4643.

Bajpai, A. K., Shukla, S. K., Bhanu, S., & Kankane, S. (2008). Reponsive polymers in controlled drug delivery. *Progress Polymer Science*, *33*, 1088–1118.

Bo, Q., & Zhao, Y. (2006). Double-hydrophilic block copolymer for encapsulation and two-way pH change-induced release of metalloporphyrins. *Journal of Polymer Science: Part A: Polymer Chemistry*, *44*, 1734–1744.

Dahmen, J., Frejd, T., Gronberg, G., Lave Thomas Magnusson, G., & Noori, G. (1983). 2-Bromoethyl glycosides: synthesis and characterization. *Carbohydrate Research*, *116*, 303–307.

Dong, C. M., Faucher, K. M., & Chaikof, E. L. (2004). Sythesis and properties of biomimetic poly(L-glutamate)-b-poly(2-acryloyloxyethyllactoside)-b-poly(L-glutamate) triblock copolymers. *Journal of Polymer Science: Part A: Polymer Chemistry*, *42*, 5754–5765.

Dong, C. M., Sun, X. L., Fancher, K. M., Apkarian, R. P., & Chaikof, E. L. (2004). Synthesis and characterization of glycopolymer-polypeptide triblock copolymers. *Biomacromolecules*, *5*, 224–231.

Ganta, S., Devalapally, H., Shahiwala, A., & Amiji, M. (2008). A review of stimuli-responsive nanocarriers for drug and gene delivery. *Journal Controlled Release*, *126*, 187–204.

Gil, E. S., & Hudson, S. M. (2004). Stimuli-responsive polymers and their bioconjugates. *Progress Polymer Science*, *29*, 1173–1222.

Hernández, J. R., Chécot, F., Gnanou, Y., & Lecommandoux, S. (2005). Toward 'smart' nano-objects by self-assembly of block copolymers in solution. *Progress Polymer Science*, *30*, 691–724.

Horgan, A. M., Marshall, A. J., Kew, S. J., Dean, K. E. S., Creasey, C. D., & Kbilan, S. (2006). Crosslinking of phenylboronic acid receptors as a means of glucose selective holographic detection. *Biosensors Bioelectronics*, *21*, 1838–1845.

Jin, X. J., Zhang, X. G., Wu, Z. M., Teng, D. Y., Zhang, X. J., Wang, Y. X., et al. (2009). Amphiphilic randomglycopolymer based on phenylboronic acid: synthesis, characterization, and potential as glucose-sensitive matrix. *Biomacromoleculars*, *10*, 1337–1345.

Lamiral, V., Melia, E., & Haddleton, D. M. (2004). Synthesis glycopolymers: an overview. *European Polymer Journal*, *40*, 431–449.

Lattuada, M., & Hatton, T. A. (2007). Functionalization of monodisperse magnetic nanoparticles. *Langmuir*, *23*, 2158–2168.

Lowe, A. B., & McCormick, C. L. (2007). Reversible addition-fragmentation chain transfer (RAFT) radical polymerization and synthesis of water-soluble (co)polymers under homogeneous conditions in organic and aqueous media. *Progress Polymer Science*, *32*, 283–351.

Li, Y. C., Larsson, E. L., Jungvid, H., Galaev, I. Y., & Mattiasson, B. (2001). Shielding of protein-boronate interactions during boronate chromatography of neoglycoproteins. *Journal of Chromatography A*, *909*, 137–145.

Li, Z. C., Liang, Y. Z., Cheng, G. Q., & Li, F. M. (2000). Synthesis of amphiphilic block copolymers with well-defined glycopolymer segment by atom transfer radical polymerization. *Macromolecular Rapid Communications*, *21*, 375–380.

Liang, Y. Z., Li, Z. C., Chen, G. Q., & Li, F. M. (1999). Synthesis of well-defined poly[(2-β-D-glucopyranosyloxy)ethyl acrylate] by atom transfer radical polymerization. *Polymer International*, *48*, 739–742.

Lu, Z. H., Liu, G. J., & Duncan, S. (2005). Morphology and permeability of membrances of polysulfone-*graft*-poly(*tert*-butyl acrylate) and derivatives. *Journal of Membrane Science*, *250*, 17–28.

Murakami, T., Hirono, R., Sato, Y., & Furusawa, K. (2007). Efficient synthesis of ω-mercaptoalkyi 1,2-*trans*-glycosides from sugar peracetates. *Carbohydrate Research*, *342*, 1009–1020.

Qureshi, S., Al-Shabanah, A., Al-Harbi, M. M., Al-Bekairi, A. M., & Raza, M. (2001). Boric acid enhances in vivo Ehrlich ascites carcinoma cell proliferation in Swiss albino mice. *Toxicology*, *165*, 1–11.

Reppy, M. A., & Pindzola, B. A. (2007). Biosensing with polydiacetylene materials: structures, optical properties and applications. *Chemical Communications*, 4317–4338.

Rijcken, C. J. F., Soga, O., Hennink, W. E., & Nostrum, C. F. (2007). Triggered destabilisation of polymeric micelles and vesicles by changing polymers polarity: an attractive tool for drug delivery. *Journal of Controlled Release*, *120*, 131–148.

Roy, D., Cambre, J. N., & Sumerlin, B. S. (2008). Sugar-responsive block copolymers by direct RAFT polymerization of unprotected boronic acid monomer. *Chemical Communications*, 2477–2479.

Storey, R. F., Scheuer, A. D., & Achord, B. C. (2005). Amphiphilic poly(acrylic acid-*b*-styrene-*b*-isobutylene-*b*-styrene-*b*-acrylic acid) pentablock copolymers from a combination of quasiliving carbocationic and atom transfer radical polymerization. *Polymer*, *46*, 2141–2152.

Tian, Y., Ravi, P., Bromberg, L., Hatton, T. A., & Tam, K. C. (2007). Synthesis and aggregation behavior of Pluronic F87/poly(acrylic acid) block copolymer in the presence of doxorubicin. *Langmuir*, *23*, 2638–2646.

Tsutsumiuchi, K., Aoi, K., & Okada, M. (1997). Synthesis of polyoxazoline-(glyco)peptide block copolymers by ring-opening polymerization of

(sugar-substituted) α-amino acid *N*-carboxyanhydrides with polyoxazoline macroinitiators. *Macromolecules*, *30*, 4013–4017.

Wang, B. L., Ma, R. J., Liu, G., Li, Y., Liu, X. J., An, Y. L., et al. (2009). Glucose-responsive micelles from self-assembly of poly(ethylene glycol)-*b*-poly(acrylic acid-*co*-acrylamidophenylboronic acid) and the controlled release of insulin. *Langmuir*, *25*, 12522–12528.

Wang, B. L., Ma, R. J., Liu, G., Liu, X. J., Gao, Y. H., Shen, J. Y., et al. (2010). Effect of coordination on the glucose-responsiveness of PEG-*b*-(PAA-*co*-PAAPBA) micelles. *Macromolecular Rapid Communications*, *31*, 1628–1634.

Winblade, N. D., Nikolic, I. D., Hoffman, A. S., & Hubbell, J. A. (2000). Blocking adhesive to cell and tissue surfaces by the chemisorption of a poly-L-lusine-*graft*-(poly(ethylene glycol); phenylboronic acid) copolymer. *Biomacromolecular*, *1*, 523–533.

Xiao, N. Y., Li, A. L., Liang, H., & Lu, J. (2008). A well-defined novel aldehyde-functionalized glycopolymer: synthesis, micelle formation, and its protein immobilization. *Macromoleculars*, *41*, 2374–2380.

Xue, Y. N., Huang, Z. Z., Zhang, J. T., Liu, M., Zhang, M., Huang, S. W., et al. (2009). Synthesis and self-assembly of amphiphilic poly(acrylic acid-*b*-DL-lactide) to form micelles for pH-reponsive drug delivery. *Polymer*, *50*, 3706–3713.

Zhao, Y. (2009). Photocontrollable block copolymer micelles: what can we control? *Journal of Material Chemistry*, *19*, 4887–4895.